The effect of stiffness of externally bonded FRP in RC beams subjected to shear

T. KANAKUBO, University of Tsukuba, Japan, T. FURUTA, Akashi National College of Technology, Japan, and H. FUKUYAMA, Building Research Institute, Ministry of Construction, Japan

INTRODUCTION

Nowadays, strengthening methods where continuous fiber laminates such as carbon, aramid, and glass are used as external seismic reinforcement for reinforced concrete (RC) structures are widely utilized. Recently, many experiments on these methods have been reported and the results of these experiments have provided some insight. However, the strength and deformation behaviour of the RC members have been predicted using existing design equations for steel rebars and by substituting the strength of the steel with that of the FRP (lateral reinforcement). Equations clarifying the actual failure mechanisms have not been reported. Most existing design equations for RC members are based on the yield strength of steel rebars and are not appropriate for elastic materials such as FRP. In addition, the failure of FRP is "fiber rupture failure" and thus brittle failures need to be considered when evaluating fiber RC members.

The final objective of study is to find an evaluation method for the ultimate strength and the deformation capacity of strengthened RC members, based on failure mechanisms. The members are reinforced using materials such as carbon or aramid fiber as externally bonded reinforcement for RC structures in seismic regions. In order to identify an appropriate analysis method, shear tests on RC members were conducted. These members were reinforced using several different types of continuous fibers (carbon, aramid, glass, and polyester). The effect of the FRP stiffness on the behavior of RC beams subjected to shear forces is thus investigated. The stiffness of FRP laminates is defined as elastic modulus (${}_fE$) × fiber thickness (${}_ft$).

OUTLINE OF EXPERIMENTS

Specimens and Materials

The specimen details are shown in Table 1 and Figure 1. The specimens are 160mm wide, 250mm high, and 750mm long, with a shear span ratio of 1.5 and a concrete strength between 30.3 and 44.2 MPa. The main steel bars are 8-D13 (p_t =1.27%, yield strength grade 800MPa) and the lateral reinforcement, D4@90 (${}_sp_w$ =0.17%, yield strength grade 295MPa). The main parameter in this study is the fiber material. As shown in Table 1, five different fibers were tested; normal carbon fiber (NCF), high elastic carbon fiber (HCF), aramid fiber (ARF), glass fiber (GLF), and polyester fiber (PAF). The elastic modulii (${}_fE$) of NCF and HCF were 240GPa and 390GPa, respectively. The reinforcing amount of FRP for all specimens was set so that the elastic modulus (${}_fE$) × fiber thickness (${}_ft$) = 20.0. Since the cross section of the specimens is constant in this study, the ratio of FRP to unit cross section (${}_fp_w$) is proportional

FRPRCS-5, Thomas Telford, London, 2001.

to the fiber thickness. Namely, ${}_fE{\cdot}{}_ft$ can be used for ${}_fE{\cdot}{}_fp_w$. The control specimen (No.1) had no FRP reinforcement, with ${}_sp_w$ =0.17%. Specimen No.2 had 150g/m^2 of NCF, No.3 93g/m^2 of HCF, No.4 242g/m^2 of ARF, No.5 698g/m^2 of GLF and No.6 727g/m^2 of PAF. The calculated bending strength for each specimen (${}_{cal}Q_{mu}$) was 167kN. All specimens were designed to obtain a shear failure at ultimate. Hence in the FRP strengthened specimens, a shear failure by fiber rupture is expected.

Table 1 List of Specimens

No.	Identification	Fiber	${}_ft$ (mm)	Layer	${}_fE$ (GPa)	${}_f\sigma_u$ (MPa)	${}_ft{\cdot}{}_fE$ (kN/mm)	${}_fp_w$ (%)	${}_fE{\cdot}{}_fp_w$ (MPa)	${}_f\sigma_u{\cdot}{}_fp_w$ (MPa)
1	N-0	-	-	-	-	-	-	-	-	-
2	NCF-150	Carbon	0.084	1	240	3400	20.0	0.104	250.5	3.55
3	HCF-93	High elastic carbon	0.051	62.5@162.5	390	2900	20.0	0.056	250.3	1.61
4	ARF-242	Aramid	0.167	150@173	120	2100	20.0	0.209	250.5	4.38
5	GLF-698	Glass	0.275	2+61.3@162	73	1470	20.0	0.344	250.9	5.05
6	PAF-727	PAF	0.501	1+(50@58.3)	40	1300	20.0	0.626	250.5	8.14

${}_f\sigma_u$: tensile strength of fiber (nominal value), ${}_fp_w$: ratio of FRP to unit cross section

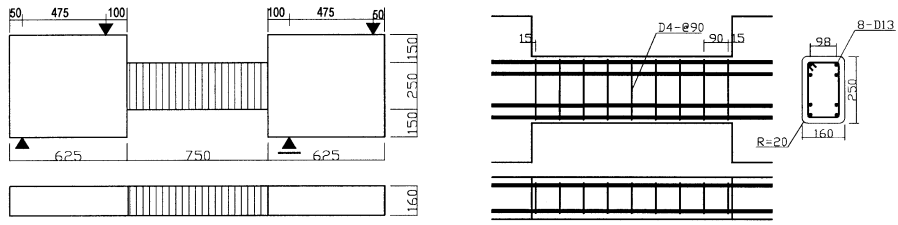

Figure 1 Specimen details (units : mm)

Loading Method and Measurements

The test apparatus and the positions of the displacement transducers are illustrated in Figure 2. The anti-symmetrical moment loading system was applied. Specimens were subjected to one way loading. The relative displacement was defined by two displacement transducers placed at the center of the beam (Figure 2). The locations of the strain gauges on the FRP and the rebars are illustrated in Figure 3.

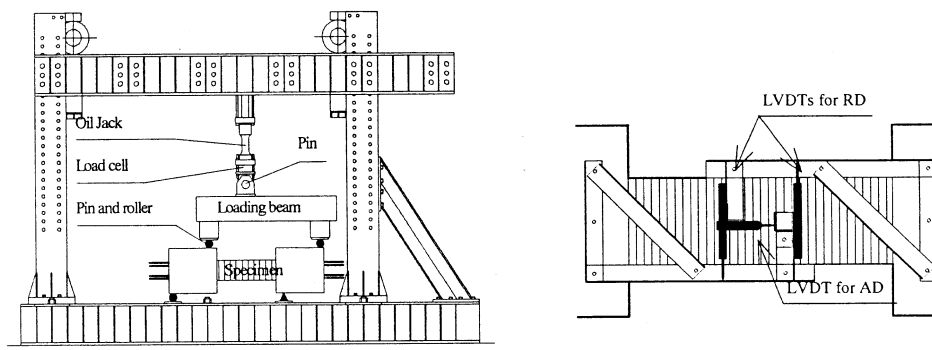

Figure 2 Loading Method

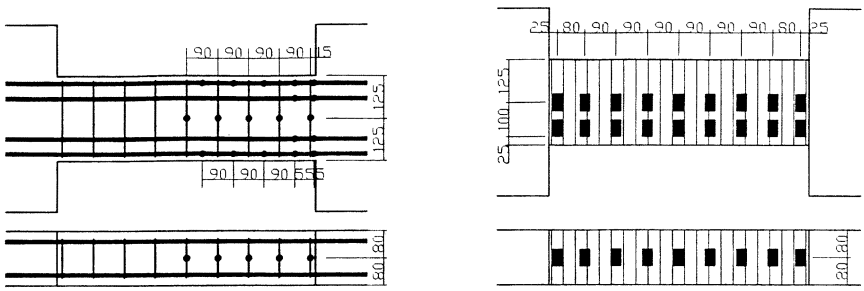

Figure 3 Locations of strain gauges (units : mm)

EXPERIMENTAL RESULTS

Failure Patterns

Figure 4 shows a diagram of the shear force (Q) versus relative displacement (δ) and typical ultimate failure patterns are indicated in Photo 1. Table 2 shows the relationship between the drift angle (R) and shear force (Q). In beam No.1, shear cracks at both ends of the beam had developed at a drift angle of (R)=1/125rad, and the lateral reinforcement had yielded. At R=1/111rad, the specimen reached the ultimate strength (Q_{max})=61.9kN. At this drift angle, the shear cracks opened widely. Simultaneously, the specimen exhibited a typical shear failure, with a sharp decrease in strength after the ultimate strength had been reached.

Except for beam No.3, the strengthened specimens were fully covered with FRP on the surface, and thus the crack patterns for these specimens were not observed. Specimens No.2, No.4, and No.5 reached Q_{max} =127.4kN (R=1/30rad), Q_{max} =124.0kN (R=1/24rad), and Q_{max} =127.1kN (R=1/22rad), respectively. After these specimens reached the ultimate strength, the FRP reinforcement ruptured, and the expected shear cracks developed rapidly. Simultaneously, the strength of the specimens decreased radically. No.3 (HCF) reached Q_{max}=127.4kN at R=1/60rad. After that, the FRP reinforcement ruptured when the shear cracks opened widely, and the strength of the specimen decreased suddenly. No.6 (PAF) reached Q_{max} =112.6kN at R=1/30rad. This specimen sustained a fairly constant load with no rupture even at the final drift angle (R=1/12rad). For specimens No.4, No.5 and No.6 it was observed that the main bars yielded after reaching the maximum strength.

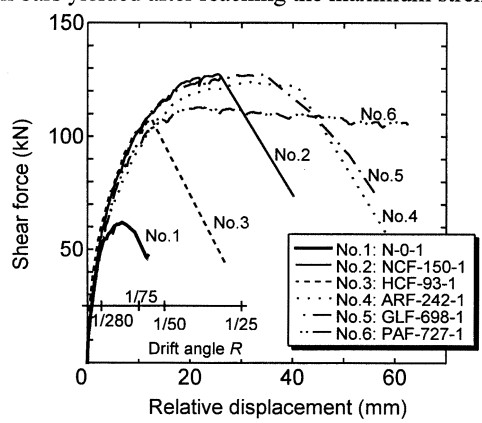

Figure 4 Shear force – relative displacement curves

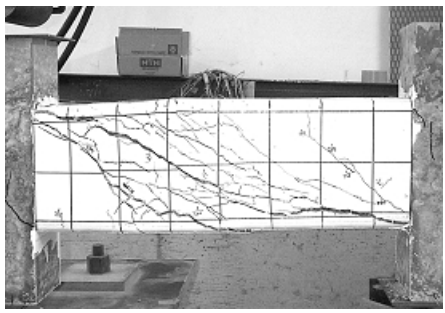

No.1 N-0

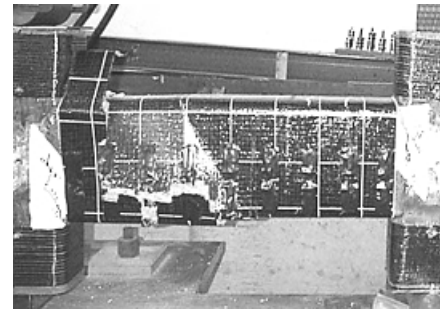

No. 2 NCF-150

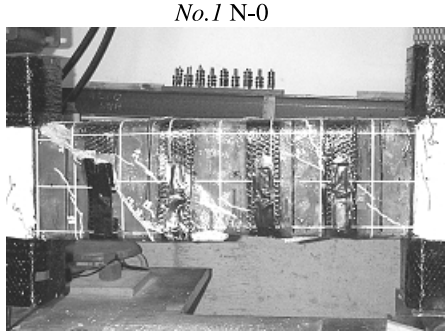

No. 3 HCF-93

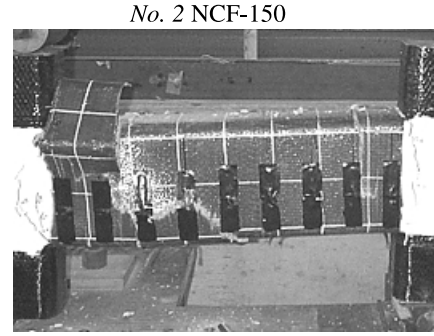

No. 4 ARF-242

Photo 1 Ultimate failure pattern

Table 2 Shear force vs drift angle

No	Identifi-cation	Max shear force Q_{max} (kN)	Drift angle at Q_{max} (rad)	Drift angle at yielding of main bars (rad)	Shear force (kN)						
					1/280	1/200	1/150	1/100	1/75	1/60	1/30
1	N-0	61.9	1/111	—	50.5	54.6	59.6	—	—	—	—
2	NCF-150	127.4	1/30	—	55.9	66.9	76.7	91.5	102.5	116.0	126.9
3	HCF-93	107.6	1/60	—	60.2	60.8	78.0	93.7	103.0	107.5	—
4	ARF-242	124.0	1/24	1/22	50.7	61.4	69.2	83.4	94.3	110.0	123.2
5	GLF-698	127.1	1/22	1/17	56.1	66.2	77.3	91.6	102.9	115.6	126.6
6	PAF-727	112.6	1/30	1/20	50.6	62.0	72.6	87.7	96.5	106.9	111.5

The location where the FRP reinforcement ruptured was the same for all strengthened specimens. The rupture occurred because the shear cracks in the concrete inside the FRP opened significantly, and the concrete was pushed out toward the FRP. In particular, the fibers were damaged and cut due to the stress concentration at a certain point in the FRP. As shown in Figure 4 and Table 2, the Q-δ relationship is similar for all specimens until around R=1/280rad, when shear cracks started to occur in beam No.1. The Q-δ relationship of the strengthened specimens is similar until around R=1/60rad, the stage when specimen No.3 reached the ultimate strength. After R=1/60rad, the Q-δ relationships of specimens No.2, No.4 and No.5 were similar and the strength increased as the deformation increased.

However, in the case of Specimen No.6 the strength was maintained after R=1/60rad and only the deformation increased.

Relationship between Shear Forces and Elastic Modulus of Fibers

Plots of the relationship between the shear force (Q) and the elastic modulus ($_fE$) and between the shear force and the FRP strength times reinforcing amount ($_f\sigma_u \cdot {}_fp_w$) at R=1/200rad, 1/100rad, 1/60rad and at the ultimate strength are illustrated in Figure 5. Both diagrams show that, at each drift angle, a similar behavior for each specimen is observed. The shear forces sustained by specimens ARF and PAF were relatively lower than those of the other specimens. In particular, the shear force increment for PAF tended to decrease with increasing deformation, when compared to the other specimens. In the case of HCF, the ultimate strength was already reached at R=1/60rad, and the ultimate strength of HCF was the lowest amongst all the strengthened specimens.

When the reinforcing stiffness of FRP ($_fE \cdot {}_fp_w$) was identical, Q_{max} for NCF, GLF and ARF were nearly the same. Considering that Q_{max} of the lower elasticity PAF and higher elasticity HCF were lower than those of NCF, GLF and ARF, it is observed that Q_{max} did not increase for a constant $_fE \cdot {}_fp_w$, when the factor $_f\sigma_u \cdot {}_fp_w$ increased.

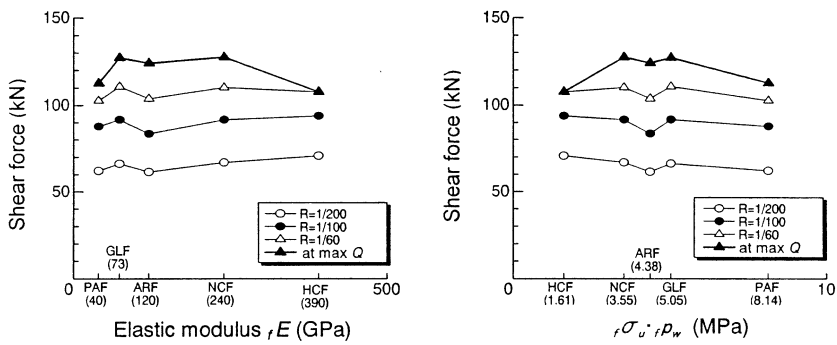

Figure 5 Shear force vs elastic modulus and strength of FRP

Strain Distributions of FRP

Figure 6 illustrates the FRP strain distribution at R=1/200rad, 1/100rad, 1/60rad, and at the ultimate load. The data points for the strain distribution are the average of two strain gauge readings at the same location along the fiber direction on the surface of each specimen (as shown in Figure 3).

The strains at R=1/200rad were very small, with an average value of approximately 220μ. The strains at R=1/100rad are more varied. The strains around 200mm from both ends of specimens at this drift angle tended to be large, with an average of about 2700μ. The average of all strains was approximately 1100μ. There was no marked difference between the different fiber types at R=1/60rad, when No.3 (HCF) had fiber rupture. All specimens showed generally the same strain distributions. The average of the strains around 200mm from both ends at R=1/60rad was about 4800μ. The global average strain was approximately 2500μ. At the ultimate load, specimen No.5 (GLF) showed the highest strain followed by, in descending

order, specimens No.4 (ARF), No.2 (NCF), No.3 (HCF) and No.6 (PAF). This order corresponded to the order of the ultimate strength. The average strain around 200mm from both ends was approximately 8200μ. The global average strain was about 6000μ.

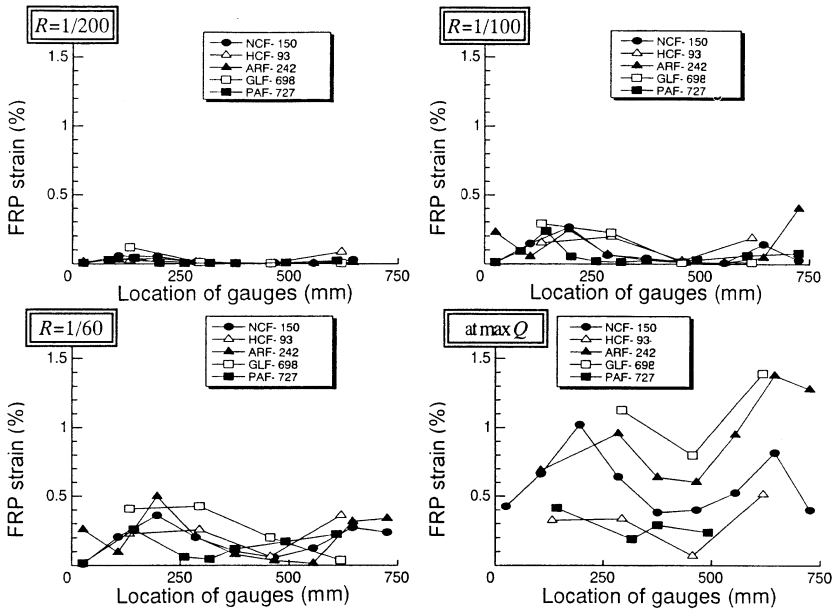

Figure 6 FRP Strain distribution

Stress of FRP

Figure 7 shows a diagram of the actual stress ($_f\sigma_s = \varepsilon \times {}_fE$) versus drift angle ($R$=1/200rad, 1/100rad, 1/60rad, and 1/30rad). The maximum values of the strains in Figure 6 are used in calculating $_f\sigma_s$. It was observed that generally the FRP in each specimen carried the same stress until R=1/60rad. The stress of specimen No.5 (GLF) at R=1/30rad (approximately when the specimen reached the ultimate strength) was the largest. The stresses of specimens No.4 (ARF), No.2 (NCF) and No.6 (PAF) were smaller in this order. In particular, the stress of No.6 was less than half that of the other specimens.

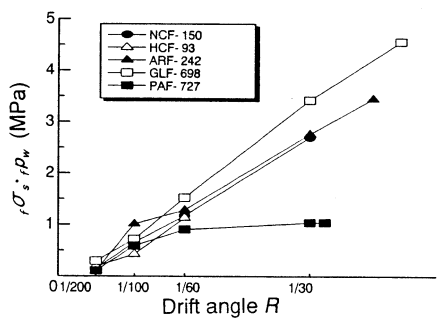

Figure 7 Actual stress of FRP vs drift angle

It was confirmed that the FRP stresses up until R=1/60rad were generally the same when the reinforcing amount of FRP was identified for a constant value of the elastic modulus ($_fE$) × fiber thickness ($_ft$). However, it appears that around R=1/30rad, there were different characteristics depending on the fiber type. It is supposed that not only the modulus of elasticity of the fiber but also parameters such as the thickness and shear capacity of the fiber caused the differences in the FRP stress in each specimen.

Shear Strength Evaluations

Table 3 compares the shear strength calculated by the Truss - Arch Method (Method A of AIJ[1]) with the experimental ultimate strength for each specimen. The following two methods of calculating the shear strengths were adopted; using the actual stress of FRP ($_f\sigma_s$: the stress calculated from the maximum strain in Figure 6), and utilizing an effectiveness coefficient, $_f\nu$=0.3, for $_f\sigma_u$.

In case of using $_f\sigma_s$, the ratio, Q_{max} / $_{cal}Q_{su}$, varied from 0.67 to 0.98. In all specimens except for No.6 (PAF), which had a low elasticity, the calculated shear strengths were noticeably higher than the actual ultimate strengths. It is supposed that the strain gauges at the location where fiber rupture occurred were significantly stressed due to the concrete cracks. When $_f\nu$ =0.3 is used, the ratio, Q_{max} / $_{cal}Q_{su}$, varied from 0.71 to 1.20, because the strengths of all different types of fiber were multiplied by the same effectiveness coefficient ($_f\nu$ =0.3). It is obvious that specific effectiveness coefficients for each different type of fiber should be proposed.

Table 3 Shear strength evaluation

No.	Identification	Q_{max} (kN)	$_{cal}Q_{f\sigma s}$ (kN)	Q_{max}/ $_{cal}Q_{f\sigma s}$	Effectiveness coefficient $_f\nu$	$_{cal}Q_{su}$ (kN)	Q_{max}/ $_{cal}Q_{su}$
2	NCF-150	127.4	136.2	0.94.	0.3	106.6	1.20
3	HCF-93	107.6	120.9	0.89		101.6	1.06
4	ARF-242	124.0	194.4	0.64		128.0	0.97
5	GLF-698	127.1	190.4	0.67		130.9	0.97
6	PAF-727	112.6	115.4	0.98		159.1	0.71

CONCLUSIONS

On the basis of this study, the following conclusions can be drawn:

1. When the reinforcing amount of FRP for each fiber type was chosen to obtain a constant stiffness (elastic modulus ($_fE$) × fiber thickness ($_ft$)) the shear force versus relative displacement curve and the relationship between the shear force and FRP stress for each specimen were generally the same, regardless of fiber type.
2. Fiber rupture occurred because the fibers became damaged and ruptured at a certain point due to stress concentrations at the location of the concrete cracks.
3. A specific effectiveness coefficient ($_f\nu$) for each different type of fiber is required to evaluate the shear strengths of RC members.

ACKNOWLEDGEMENTS

This study was conducted under the University of Tsukuba Research Project. The authors also acknowledge Chikara Iihoshi from Asahi Chemical Industry Co., Keisuke Takahashi from Mitsubishi Chemical Functional Products Inc., and Masaharu Tanigaki from Mitsui Construction Co.

NOTATION

$_fE$: elastic modulus of fiber
p_t : main bar ratio
$_fp_w$: reinforcement ratio for fiber
$_sp_w$: lateral reinforcement ratio for steel rebar
Q : shear force
$_{cal}Q_{f\sigma s}$: calculated shear strength using $_f\sigma_s$
Q_{max} : maximum shear force
$_{cal}Q_{mu}$: calculated bending strength (in shear force)
$_{cal}Q_{su}$: calculated shear strength using $_f\nu$
R : drift angle
$_ft$: thickness of fiber
$_f\nu$: effectiveness coefficient for FRP
$_f\sigma_s$: experimental obtained stress of FRP
$_f\sigma_u$: tensile strength of fiber

REFERENCES

1) Architectural Institute of Japan : Design Guidelines for Earthquake Resistant Reinforced Concrete Buildings Based on Ultimate Strength Concept, pp.106 – 116, 1990